

# Crystal–solvate phases of poly(*p*-phenylene benzobisoxazole)

Yachin Cohen\*

Department of Chemical Engineering, Technion-Israel Institute of Technology, Haifa 32000, Israel

and W. Wade Adams

Wright Laboratory, Materials Directorate, Wright-Patterson AFB, OH 45433, USA

(Received 26 April 1995)

The crystal structure and morphology in oriented solutions of the rigid polymer poly(*p*-phenylene benzobisoxazole) (PBZO) in polyphosphoric acid (PPA), at different degrees of exposure to moisture, were studied by transmission electron microscopy and X-ray diffraction. Two crystal solvate forms, crystalline complexes of PBZO and PPA, were found. The form I crystal solvates exhibit several sharp equatorial reflections, whereas only a few broad reflections are observed in the form II state. All crystal solvate phases studied exhibit three-dimensional crystallinity evident in sharp off-meridional reflections. This is considered to be due to unique associations between the protonated PBZO polycations and the PPA anions. Endothermic transitions observed upon heating the crystal solvates are interpreted as dissolution of the form I crystals at about 70°C and crystal–crystal transformation of the form II crystal solvate to PBZO crystals, due to deprotonation above 300°C. A microfibrillar morphology is observed in the oriented PBZO fibre coagulated by immersion in water. Similar microfibrils, less than 10 nm in width, are already observed in the form II crystal solvate state, obtained from the oriented solution by absorption of moisture. Copyright © 1996 Elsevier Science Ltd.

(Keywords: rigid polymer; crystallization; crystal–solvate)

## INTRODUCTION

Exceptionally high tensile properties can be attained in polymeric materials when the polymer chain is fully extended. One way for achieving this is by synthesis of rigid chain polymers, such as the aromatic heterocyclic polymers developed by the US Air Force Ordered Polymers Program. The rigidity and regularity of the molecular structure along the chain render these polymers processable only from solutions in strongly interacting solvents, such as strong acids. A high degree of orientational order of the rigid chains, achieved during processing of fibres from solutions, leads to tensile modulus and strength exceeding 300 and 3 GPa, respectively<sup>1</sup>. Two examples from this group of rigid polymers are *trans*-poly(*p*-phenylene benzobisthiazole) (PBZT), the properties and structure of which have been studied extensively during the last decade, and *cis*-poly(*p*-phenylene benzobisoxazole) (PBZO), studies on which have been reported more recently<sup>1</sup>. The chemical structures of PBZT and PBZO are shown in *Figure 1*. Often the solvent used for processing these polymers is poly(phosphoric acid) (PPA), which is their polymerization medium<sup>2</sup>. In a typical process for spinning rigid polymer solutions, a liquid crystalline solution is extruded through a spinnerette separated by a narrow

air-gap from a coagulation bath. The elongational flow field in this air-gap results in a high degree of chain orientation. Solidification of the solution stream occurs in the coagulation bath by the action of a non-solvent, typically water. The oriented liquid crystalline solution of the protonated rigid polymer in its acid solvent is transformed during coagulation to the crystalline (solid) state, following deprotonation of the polymer by the coagulant.

Intermediate crystalline phases in systems composed of rigid polymer, acid solvent and water coagulant have been pointed out in recent years, as described initially by Papkov and co-workers<sup>3</sup>. These are the so-called crystal–solvate phases which result from co-crystallization of the polymer with its solvent. Studies on oriented solutions of PBZT in polyphosphoric acid (PPA)<sup>4–6</sup> revealed that two types of crystal–solvate phases exist in these systems. The first type, denoted form I, is a highly ordered crystalline phase, exhibiting three-dimensional order usually absent in the solid PBZT crystalline state. It appears at low moisture uptake by the PBZT/PPA solution, has a light-green colour and is considered as a co-crystal of protonated PBZT cations and PPA anions. At higher moisture uptake, or when the solution stream is coagulated in 85% phosphoric acid, another type of crystal solvate phase appears. It is denoted form II, has a reddish colour, and is much less ordered than the form I crystal

\* To whom correspondence should be addressed

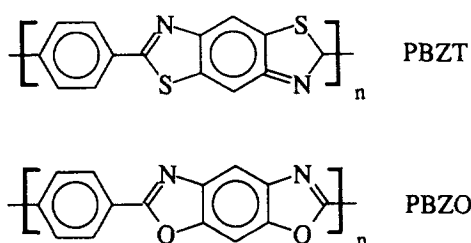


Figure 1 The chemical structures of *trans*-PBZT and *cis*-PBZO

solvate. In a preliminary report, crystal solvate phases of PBZO in PPA were described<sup>4</sup>. The general behaviour was similar to the case of PBZT/PPA, in that both highly ordered (form I) and less ordered (form II) crystal solvates were observed. However, there was no change in colour upon transition between the crystal solvate forms, and the form II crystal maintained three-dimensional order. The objective of this report is to describe the structures of the different crystal solvate forms of PBZO/PPA and to discuss differences between this system and that of PBZT/PPA described elsewhere<sup>4-6</sup>. Studies on the transformation between the different phases by X-ray diffraction using synchrotron radiation were also reported elsewhere<sup>6</sup>.

Recent studies on the crystal structure of PBZO fibres by X-ray diffraction (XRD)<sup>7</sup> and transmission electron microscopy (TEM)<sup>8</sup> revealed the packing of PBZO molecules in a monoclinic non-primitive unit cell containing two chains, and single-crystal texturing was observed in thin films detached from PBZO fibres<sup>8,9</sup>. It was concluded that neighbouring chains along the *a* direction are displaced relative to each other by an axial shift of  $1/4c$ . The development of three-dimensional crystallinity in heat-treated fibres was determined from the observation of a strong off-meridional reflection, indexed as (302)<sup>8</sup>. The microstructure was studied by TEM<sup>8-11</sup>, providing direct evidence for the high degree of local orientational order as well as the extent of lateral and axial order in the packing of the polymer chains. A domain morphology of uniaxially oriented small crystallites of dimensions ranging from 8 to 20 nm even after heat treatment, deduced by Martin and Thomas based on high resolution TEM, emphasized the importance of defects such as grain boundaries and dislocations in control of material properties<sup>8</sup>. The reason for the limited size of the PBZO crystallites, even after heat treatment at 665°C, is unclear. It should be noted, however, that the lateral sizes reported for the crystallites are comparable to the lateral width of the microfibrils observed in PBZT fibres<sup>12,13</sup>, where the microfibrillar morphology develops during coagulation of the oriented polymer solution. A critical evaluation of possible mechanisms for the phase transformation during coagulation has recently been presented<sup>14</sup>. It is plausible that boundaries of the microfibrils, set in during coagulation, limit the growth of crystallites during subsequent heat treatment. Thus, a further aim of this study is to investigate the formation of microfibrils in oriented PBZO/PPA solutions, in relation to transitions between the crystal solvate phases.

## EXPERIMENTAL

*cis*-PBZO was obtained from Dow Chemical Co. as

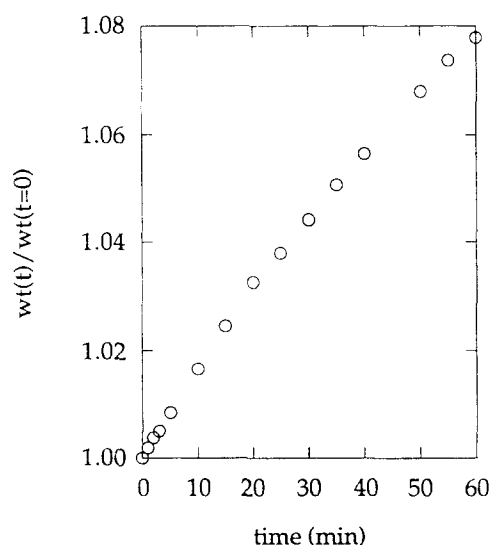


Figure 2 The increase in weight with time of a PBZO/PPA sample absorbing atmospheric moisture

solution containing 14% by weight polymer in PPA (82.6%  $\text{P}_2\text{O}_5$ ). The intrinsic viscosity in methanesulfonic acid (MSA) was reported to be  $250 \text{ cm}^3 \text{ g}^{-1}$ . The PBZO/PPA solution is solid at room temperature. Samples were heated to about 60°C in a glove bag under dry nitrogen and oriented by manual extension ( $4-6 \times$  draw ratio), to form thin fibre-like samples. For exposure to moisture, a sample of 0.1–0.2 g was transferred to a thin-walled glass capillary (Müller) and exposed to ambient air. The gain in weight, monitored gravimetrically by a Sartorius AC210P balance, is an indication of the water content in the exposed samples. The capillaries were then sealed by epoxy glue for X-ray diffraction measurements. An example of a moisture uptake measurement is shown in Figure 2.

Wide-angle diffraction patterns, at room temperature, were obtained using a Warhus camera (Blake Industries Inc.) mounted on a Rigaku RU-200 generator operated at 60 kV and 200 mA.  $\text{CuK}\alpha$  radiation was used and a graphite crystal monochromator was employed. Some measurements were made with a similar set-up using a sealed tube generator (Philips PW1730). Silicon powder was used for calibration of sample-to-film distance. The scattering patterns were recorded either on Kodak DEF or Osray C film. For differential scanning calorimetry (d.s.c.) measurements a Mettler TA3000 instrument was used. Special flame-sealed glass containers (Mettler) were used for the acid-containing samples. The heating rate was  $10^\circ\text{C min}^{-1}$ .

Samples for TEM were prepared by two different techniques. For fibres coagulated in water, an impregnation procedure with low viscosity epoxy resin was used, as described previously<sup>12,13</sup>. The impregnated fibre was microtomed longitudinally with a diamond knife (Diatome) in a Reichert FC4 ultramicrotome, at room temperature. For observing the structures in the PBZO/PPA solutions, a freeze-fracture replicating technique was employed. An oriented sample was notched parallel to the draw direction, frozen in liquid nitrogen and fractured by pulling the notched fibre. The sample was then mounted in an Edwards evaporator on a copper rod cooled by circulation of boiling nitrogen. A replica of the fractured surface was created by shadowing with

platinum at 45° to the fractured surface, and deposition of a carbon support film by evaporation. The replica was released by immersion in hot MSA and subsequently washed with sulfochromic acid and distilled water. It was then picked up on a sandwich-type electron microscope grid, due to poor adhesion. The TEM samples were

viewed in a JEOL 100CX electron microscope operated at 100 kV.

### RESULTS AND DISCUSSION

Wide-angle X-ray diffraction patterns from oriented

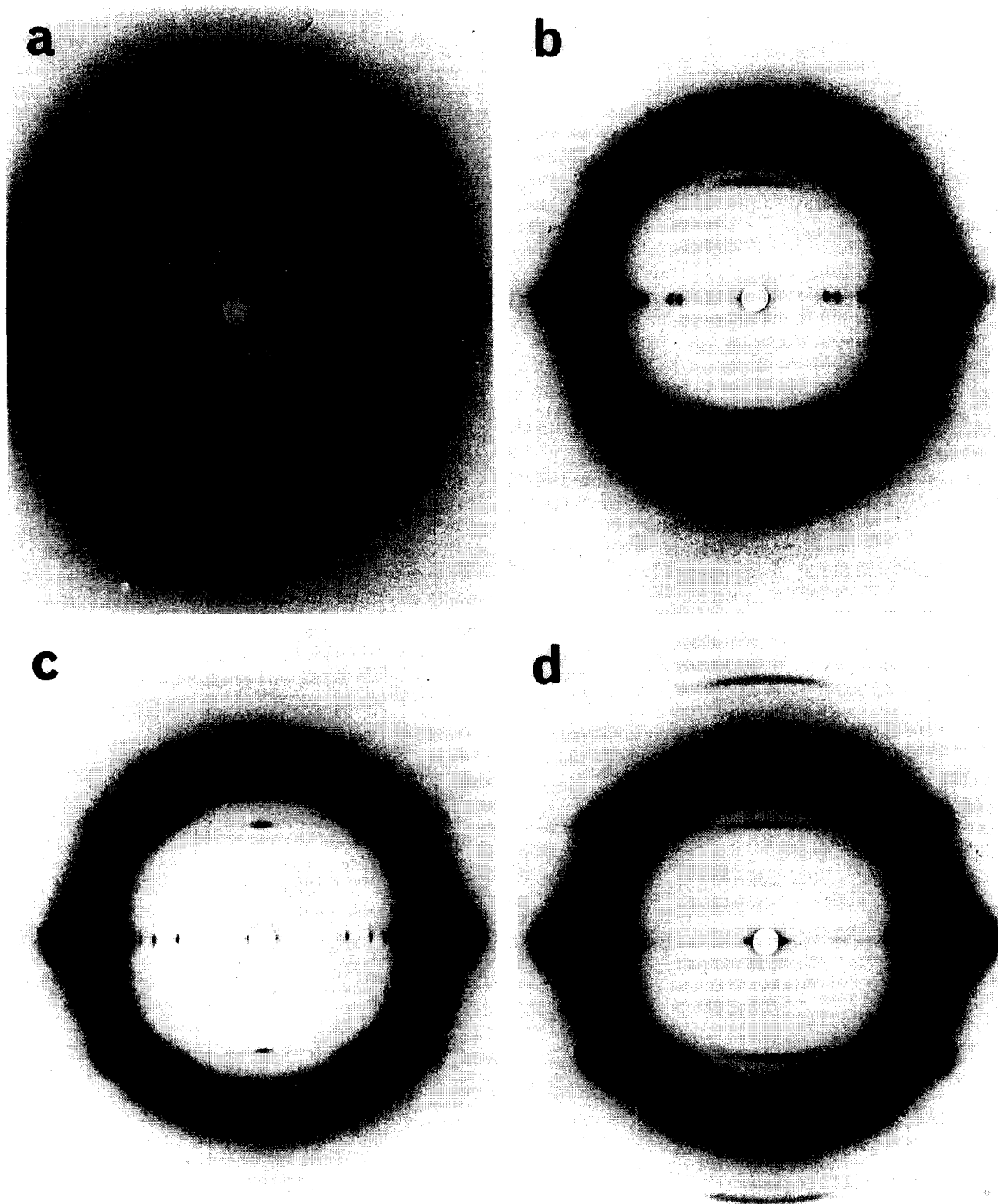


**Figure 3** The X-ray diffraction patterns from oriented PBZO/PPA samples. Form I phases: (a) in the initial dry state; (b) having absorbed moisture to 1% by weight; (c) having absorbed moisture to 7%, then exposed to vacuum for moisture reduction to about 4%. (d) The form II phase after absorption of moisture to 7% by weight

PBZO/PPA samples at different levels of exposure to moisture are shown in *Figure 3*. The samples were tested at a temperature of  $23 \pm 2^\circ\text{C}$ . Superposition of a highly oriented crystalline fibre pattern with an amorphous halo is observed in these patterns, indicating the coexistence of an oriented crystalline phase with an amorphous solution phase. A similar observation was previously made in PBZT/PPA solutions exposed to moisture<sup>5</sup>. However, no crystallization occurred in dry PBZT/PPA solutions at room temperature, although polymer concentration and intrinsic viscosity were similar in both studies. This comparison indicates that in dry PPA solutions, at the temperature and concentration reported above, PBZO crystallizes whereas PBZT remains in solution. The viscous solutions are oriented by the uniaxial stretching, and relaxation of orientation at room temperature is extremely slow, as reported by Feijoo *et al.*<sup>15</sup>. In the patterns shown in *Figure 3* several crystalline reflections on the equator are superimposed on the amorphous halo, preventing accurate assessment of the orientation of the amorphous phase.

The moisture content of the samples giving rise to the diffraction patterns shown in *Figure 3* is low. *Figure 3a* is the pattern obtained from the dry solution after orientation. Absorption of moisture to a content of about 1% (w/w) gives rise to the pattern shown in *Figure 3b*. Further absorption of moisture, to a level of about 7%, results in the pattern depicted in *Figure 3d*. When the latter sample was exposed to vacuum for several hours, during which moisture was removed to approximately 4%, the diffraction pattern reverted to the one shown in *Figure 3c*. The diffraction patterns in *Figures 3a-c* have some common features. They exhibit several sharp equatorial reflections as well as off-meridional reflections on the second layer line. Similar features were also observed in the diffraction pattern from the form I crystal solvate phase in PBZT/PPA solutions<sup>4,5</sup>. Moreover, the crystalline reflections observed in *Figures 3a-c* are sharper and exhibit a much higher degree of orientation than was achieved with the PBZT/PPA solutions<sup>4,5</sup>. The equatorial reflections of the diffraction patterns shown in *Figures 3a-c*

are listed in *Table 1*. It can be seen that additional reflections are observed in *Figures 3b* and *c*, as compared to the dry PBZO/PPA solution (*Figure 3a*). Despite these differences, we consider the crystalline state giving rise to the diffraction patterns of *Figure 3a-c* as a form I crystal solvate of PBZO/PPA.

When the PBZO/PPA solution absorbed moisture to a content exceeding 7% by weight, another crystalline form emerges, the diffraction pattern from which is shown in *Figure 3d*. Instead of having several sharp equatorial reflections, as in the form I state, only a few broad reflections are observed. Although this situation parallels the distinction made between forms I and II of the crystal solvate phases of PBZT/PPA<sup>4-6</sup>, in the case of PBZO/PPA several off-meridional reflections are observed (*Figure 3d*). We denote this phase as the form II crystal solvate of PBZO/PPA, noting that its three-dimensional order is maintained, contrary to the case of PBZT/PPA<sup>4,5</sup>. The transition to the form II state was estimated previously by indirect measurements to occur at about 5% moisture content<sup>6</sup>. Direct gravimetric measurements presented here show the transition at about 7% moisture. The transitions between the different phases encountered in the PBZT/PPA system during absorption of moisture were accompanied by changes in colour<sup>4,5</sup>. The dry solution was dark green, which turned to light green upon precipitation of the form I crystal solvate. The transition to the form II crystal solvate was marked by a change in colour to dark red. However, no colour change was observed in the transition between the crystal solvate phases of PBZO/PPA. The dry solution, as well as the crystal solvate forms I and II, exhibiting the diffraction patterns shown in *Figure 3* had a dark blue-green colour. Furthermore, the form II phase was stable during exposure to moisture for several hours. The sample appeared to exude a clear liquid, presumably PPA/water, yet neither its colour nor diffraction pattern were changed.

The differences between the phase behaviour of PBZT<sup>4,5</sup> and PBZO upon absorption of water, are summarized below.

1. In the transition from the liquid crystal solution to form I and form II crystal solvates, the PBZT system changes colour from dark green to light green, then to red. No change in colour is observed in the PBZO system.
2. The dry PBZT/PPA solution at 14% (w/w) is in the liquid crystal state, whereas a solution PBZO having comparable concentration and intrinsic viscosity is in the form I crystal solvate state.
3. The form II phase of PBZO/PPA exhibits sharp off-meridional reflections, whereas that of PBZT/PPA does not.
4. The sharp off-meridional reflections in the crystal solvate appear on a layer line which has different meridional spacings in the two systems. In the PBZO case this spacing, 0.61 nm, equals half the monomer repeat length. In the PBZT case, the layer line spacing, 0.465 nm, is three-eighths of the monomer repeat length.

The first three differences indicate that the interaction between the rigid polymer and its solvent PPA are stronger in the case of PBZO than in PBZT, suggesting that in the form II phase PBZO is still protonated

**Table 1** The spacings of the observed equatorial reflections from the form I phases in *Figure 3* (nm)

<i>Figure 3a</i>	<i>Figure 3b</i>	<i>Figure 3c</i>
0.918 s	0.915 s	0.885 w
	0.787 m	0.780 s
	0.623 m	0.616 s
0.579 s	0.580 vs	-
		0.552 w
	0.488 m	0.486 s
0.458 vs	0.455 vs	-
	0.416 m	0.424 vs
0.409 vs	0.407 vs	0.409 vs
	0.393 m	0.390 vs
0.358 vs	0.358 vs	-
	0.346 m	0.350 vs
0.314 m	0.312 w	-
0.305 m	0.303 w	0.298 vw
0.289 m	0.286 w	0.291 vw
	0.275 vw	0.272 vw
	0.262 vw	0.260 vw
0.259 w	0.256 vw	-

vs, very strong; s, strong; m, medium; w, weak; vw, very weak

**Table 2** The observed and calculated  $d$ -spacings of the reflections from the form I phase. Unit cell dimensions:  $a = 1.26$  nm,  $b = 1.16$  nm,  $c$  (chain axis) = 1.22 nm,  $\gamma = 98^\circ$ 

$d$ , obsd (nm)	$d$ , calcd (nm)	Index
Equatorial reflections		
0.915	0.911	$\bar{1}10$
0.787	0.789	110
0.623	0.623	200
0.580	0.584	$\bar{2}10$
	0.572	020
0.488	0.494	120
0.455	0.455	220
0.416	0.416	300
0.407	0.410	$\bar{3}10$
0.393	0.394	220
0.358	0.351	130
0.346	0.348	$\bar{2}30$
0.312	0.312	400
	0.312	410
0.303	0.306	$\bar{3}30$
	0.304	230
0.286	0.288	040
	0.286	$\bar{1}40$
0.275	0.275	$\bar{2}40$
0.262	0.264	330
	0.260	430
0.256	0.259	420
	0.253	$\bar{3}40$
Off-meridional reflections		
0.503	0.506	$\bar{1}12$
0.440	0.435	202
0.411	0.417	022
0.383	0.383	122
0.368	0.365	$\bar{2}22$
0.352	0.343	302
Layer-line spacings		
1.214	1.217	001
0.606	0.608	002
0.404	0.406	003

whereas PBZT is not. The last point may suggest a difference in structure or conformation of the PPA solvent in the crystal solvate.

The number of reflections observed in the diffraction patterns of the different phases allows determination of the crystal unit cell. The patterns index on a monoclinic unit cell. For the form I patterns, the smallest monoclinic unit cell which fits the reflections of the dry sample, shown in *Figure 3a*, also fits all reflections of *Figure 3b*. This supports the conclusion that both patterns are from the same form I crystal solvate phase. The unit cell dimensions are:  $a = 1.26$  nm,  $b = 1.16$  nm,  $c$  (chain axis) = 1.22 nm,  $\gamma = 98^\circ$ . The reflections and the assigned indices are listed in *Table 2*. The observation of additional reflections in *Figure 3b* may be due to structural changes of PPA which lead to loss of extinction conditions. The additional equatorial reflections in *Figure 3c* could not be fitted by the same unit cell. It is plausible that during the lengthy process of moisture absorption and its removal under vacuum, irreversible changes in the structure of PPA could have occurred, for example due to hydrolysis.

Strong off-meridional reflections appear in the diffraction patterns from the PBZO/PPA crystal solvates on the second layer line at meridional spacings of 0.61 nm. In the PBZT/PPA/water system such reflections were observed only in the form I phase, and appeared on a layer line at a meridional spacing of 0.465 nm, which did

not coincide with a PBZT layer line<sup>4,5</sup>. It was thus found necessary to invoke an axial periodicity which differs from the repeat length of the PBZT chain. The strong off-meridional reflections were assumed to arise from lattice planes containing a high concentration of phosphate groups. The particular axial periodicity of 0.465 nm was attributed to an extended conformation of the PPA chains aligned parallel to PBZT in the unit cell. Following the same reasoning, the phosphate groups in the PBZO crystal solvates may be arranged about the polymer chain with an axial repeat of 0.61 nm, half the PBZO repeat length. It should be noted that although the  $P_2O_5$  content of PPA in the polymer solutions, as reported by their suppliers, was nearly identical in both studies of PBZT<sup>4,5</sup> and PBZO, there are no actual data on the degree of polymerization of phosphate groups in the PPA solutions and in the crystal-solvate unit cells. Since the scattering patterns from the PBZO/PPA crystal solvates do not introduce a new axial repeat length, it is not necessary to make any assumption about polymerization of phosphoric acid. Furthermore, an axial repeat of 0.61 nm is larger than can be obtained by an extended 2/1 helical conformation of PPA<sup>16</sup>.

The dimensions of the unit cell determined for the form I crystal solvate of PBZO/PPA are large, indicating that it contains several PBZO chains and many phosphate groups. The stoichiometry of the crystal solvate phases, defined as the number of phosphate groups per PBZO repeat unit, cannot be determined directly. Recent studies on crystal solvates of PBZT with MSA indicate that four acid molecules are complexed with a polymer repeat unit<sup>17</sup>. Similarly, we assume that four phosphate groups are associated with each PBZO repeat unit. Furthermore, the studies on the PBZT/PPA<sup>5</sup> and PBZT/MSA<sup>17</sup> systems suggested that additional acid molecules, not directly involved in protonation of the polymer, may exist in the unit cell of the form I phase. A number of acid molecules larger than required for polymer protonation was also found in the crystal solvate of poly(*p*-phenylene terephthalamide)/sulfuric acid<sup>18</sup>. An estimated upper limit for the composition of the form I phase, compatible with the unit cell dimensions, is thus four PBZO chains and 16 phosphate groups, a composition of 42% PBZO having a crystal density of 2.1 g cm<sup>-3</sup>. The lower limit is estimated assuming two PBZO chains and 24 phosphate groups, a composition of 20% PBZO having a crystal density of 2.3 g cm<sup>-3</sup>.

The reflections from the form II crystal solvate phase, shown in *Figure 3d*, index on a monoclinic unit cell of dimensions:  $a = 0.70$  nm,  $b = 0.58$  nm,  $c$  (chain axis) = 1.20 nm,  $\gamma = 99^\circ$ . The reflections and the assigned indices are listed in *Table 3*. Studies of the crystal solvates of PBZT with PPA<sup>5</sup> and MSA<sup>17</sup> indicated that the polymer is deprotonated in the form II phase. In this study, the lack of a colour change upon transition to this phase, and the strong off-meridional reflections observed in its diffraction pattern, indicate that PBZO may still be protonated in the form II phase. If so, charge neutrality requires that PPA anions also exist in the unit cell. Under the assumption that the degree of protonation remains four per PBZO repeat unit, as discussed for the form I phase, we suggest a unit cell containing one PBZO repeat unit and four phosphate groups, with a density of 2.0 g cm<sup>-3</sup>. It is interesting to note that taking half the unit cell, in the  $a$  direction results in dimensions not much

**Table 3** The observed and calculated *d*-spacings of the reflections from the form II phase. Unit cell dimensions: *a* = 0.70 nm, *b* = 0.58 nm, *c* (chain axis) = 1.20 nm,  $\gamma = 99^\circ$ 

<i>d</i> , obsd (nm)	<i>d</i> , calcd (nm)	Index
Equatorial reflections		
0.481	0.480	110
0.350	0.346	200
0.332	0.332	210
0.289	0.286	020
0.262	0.251	120
Off-meridional reflections		
0.450	0.452	102
0.373	0.374	112
0.337	0.338	112
Layer-line spacings		
1.198	1.195	001
0.599	0.598	002
0.396	0.398	003
0.296	0.299	004

different from a primitive unit cell suggested<sup>7</sup> for the PBZO crystal (*a* = 0.560 nm, *b* = 0.354 nm, *c* = 1.205 nm,  $\gamma = 101.2^\circ$ ). This may be due to the fact that the volume of a PPA chain containing four phosphate groups, estimated as about 0.198 nm<sup>3</sup> based on the crystal structure of rubidium polyphosphate<sup>19</sup>, is comparable to the volume occupied by a PBZO repeat unit in its unit cell, 0.234 nm<sup>3</sup>. However, at this stage the diffraction data alone cannot rule out the possibility that the form II crystal contains just two PBZO chains, without PPA.

The transformations of the PBZO/PPA crystal solvate phases upon heating lead to the d.s.c. traces presented in *Figure 4*. Significant differences were observed in the behaviour of the different crystal solvate forms. *Figure 4a* is the first heating scan of PBZO/PPA in the form I state, whereas *Figure 4b* is due to the form II state. The form I phase exhibits an endothermic transition at 70°C, with an enthalpy of 4.9 J g<sup>-1</sup>. The form II phase is stable to higher temperatures, and exhibits an endothermic transition at 320°C, with an enthalpy of 20 J g<sup>-1</sup>. It should be noted that the actual weight fraction of the crystal solvate phase in the sample is not known. After heating the form I sample to 170°C and the form II sample to 370°C, cooling scans were carried out at a rate of 20°C min<sup>-1</sup>. Exothermic transitions were not observed in the cooling scans. However, both endothermic transitions were reproducible and reversible. When reheated after cooling, the transitions in both samples were evident, although with somewhat broader peaks. Similar observations were made in both cases on the third heating scan. No transitions other than the one at 70°C were observed in d.s.c. traces of the form I phase, upon further heating to 370°C. The transitions shown in *Figure 4* were not observed when a PPA/water mixture was heated in the same temperature range. However, one should bear in mind the chemical transformations which occur in the PPA/water system upon heating<sup>20</sup>. While hydrolysis of PPA is effected by the presence of water, neat PPA polymerizes at elevated temperatures, releasing water. The role of these reactions in the observed transitions is not clear.

The nature of the transitions of the crystal solvate phases can be evaluated in conjunction with diffraction measurements as a function of temperature using

synchrotron radiation<sup>6</sup>, as summarized below. The crystalline reflections from the dry form I phase were shown to gradually decrease in intensity until an amorphous pattern was obtained at 72°C. This was interpreted as melting of the PBZO/PPA form I crystal solvate into the liquid crystal state. It was also shown that the form I phase recrystallizes upon cooling. In agreement with the d.s.c. results from the form II phase, no appreciable change in the diffraction pattern was observed up to 250°C. At higher temperatures the off-meridional reflections on the second layer line faded. Along the equator, the first reflection at a spacing of 0.45 nm shifted to smaller angles reaching a spacing of 0.56 nm above 300°C, and a new reflection appeared at a spacing of 1.07 nm. This transition was interpreted as a crystal-crystal transformation between the form II state, in which PBZO is protonated and complexed with PPA anions, and the crystalline PBZO state, brought about by deprotonation of PBZO at elevated temperatures<sup>6</sup>. The three dimensional order, brought about by the specific interactions between PBZO and PPA, is lost in this transition. The lower enthalpy of transition of the form I phase at 70°C, in comparison with that of the form II phase at 320°C, is in accord with the proposition of the former being dissolution of the crystal solvate which maintains protonation of PBZO, and the latter resulting from deprotonation. It is important to note that the structure represented by the form II state, which exists already at moderate moisture uptakes by the PBZO/PPA solution, persists at temperatures much above those at which PBZO fibres are spun in practical application.

The microstructure which developed when the oriented PBZO/PPA solution was coagulated by immersion in water, as occurs in the conventional fibre-spinning process, is shown in *Figure 5*. The dark longitudinal striations are microfibrils of crystalline PBZO, the diameter of which appears to be smaller than 10 nm. The lighter background is the epoxy resin used for impregnation and fixation of the wet-coagulated fibre. The images viewed in microtomed sections, as shown in the micrograph in *Figure 5*, were very similar to those observed in PBZT fibres prepared in a similar way<sup>12,13</sup>. This network of oriented microfibrils was postulated to be the basic structural element of rigid rod fibres. It is thus of interest to investigate at what level of coagulation of a PBZO/PPA solution this microstructure emerges.

The structure of the oriented PBZO/PPA solution in the form I state, as seen in the freeze-fracture replica, is shown in *Figure 6a*. It appears featureless, with the possible exception of low contrast inhomogeneities several hundred angstroms in size. Since the diffraction pattern from this phase (*Figure 3a*) indicated coexistence of two phases, amorphous and crystalline, these results suggest that the form I phase is composed of relatively large crystallites, the density of which is comparable to that of the surrounding solution. When this phase is transformed to the form II state by absorption of moisture, a microfibrillar morphology develops, as shown in *Figure 6b*. The width of the microfibrils is about 5 nm, and they are oriented along the draw direction. In the structures proposed above for the crystal solvates of PBZO/PPA, the form I crystal contains significantly more acid than form II. Therefore acid is excluded from the crystal in the transition from the form I state

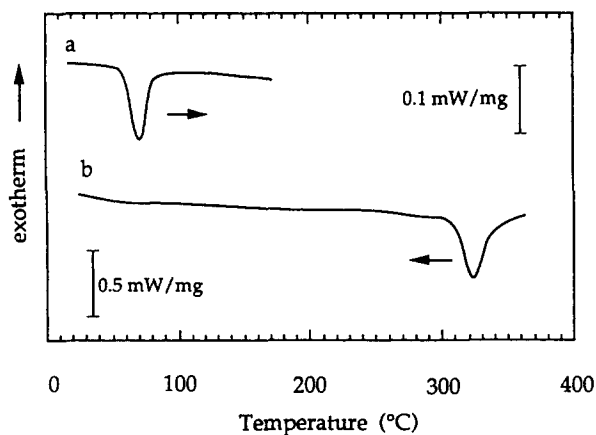


Figure 4. D.s.c. traces of the first heating scans of PBZO/PPA crystal solvates: (a) in the form I state; (b) in the form II state

(Figure 5a) to the form II state (Figure 5b). This may result in break-up of the form I crystals to smaller microfibrils, also amplified by fracture, shadowing and replication in the preparative procedure for electron microscopy. Ribbon-like microfibrils have been observed in row-nucleated structures which developed during coagulation of oriented PPTA/sulfuric acid<sup>21,22</sup> and PBZT/PPA solutions<sup>21</sup>. Collapse of the polymer-solvent complex, when solvent is excluded from the crystal solvate, was suggested as one possible origin of this microstructure. The microfibrillar morphology which develops in the form II state by absorption of a relatively small amount of moisture may be the origin of the microfibrillar morphology observed in fibres obtained from rigid polymer solutions by coagulation in water.

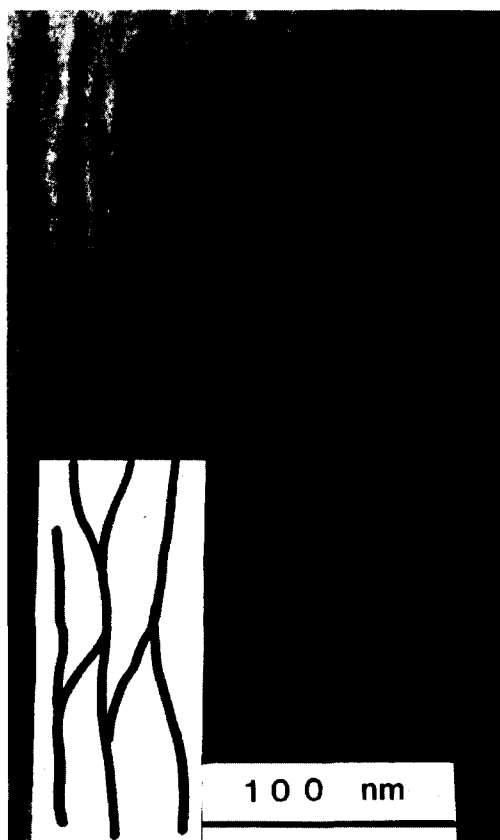


Figure 5. Electron micrograph of a microtomed section of the PBZO/PPA solution coagulated in water and impregnated with epoxy resin. Inset: a sketch of the microfibrillar network

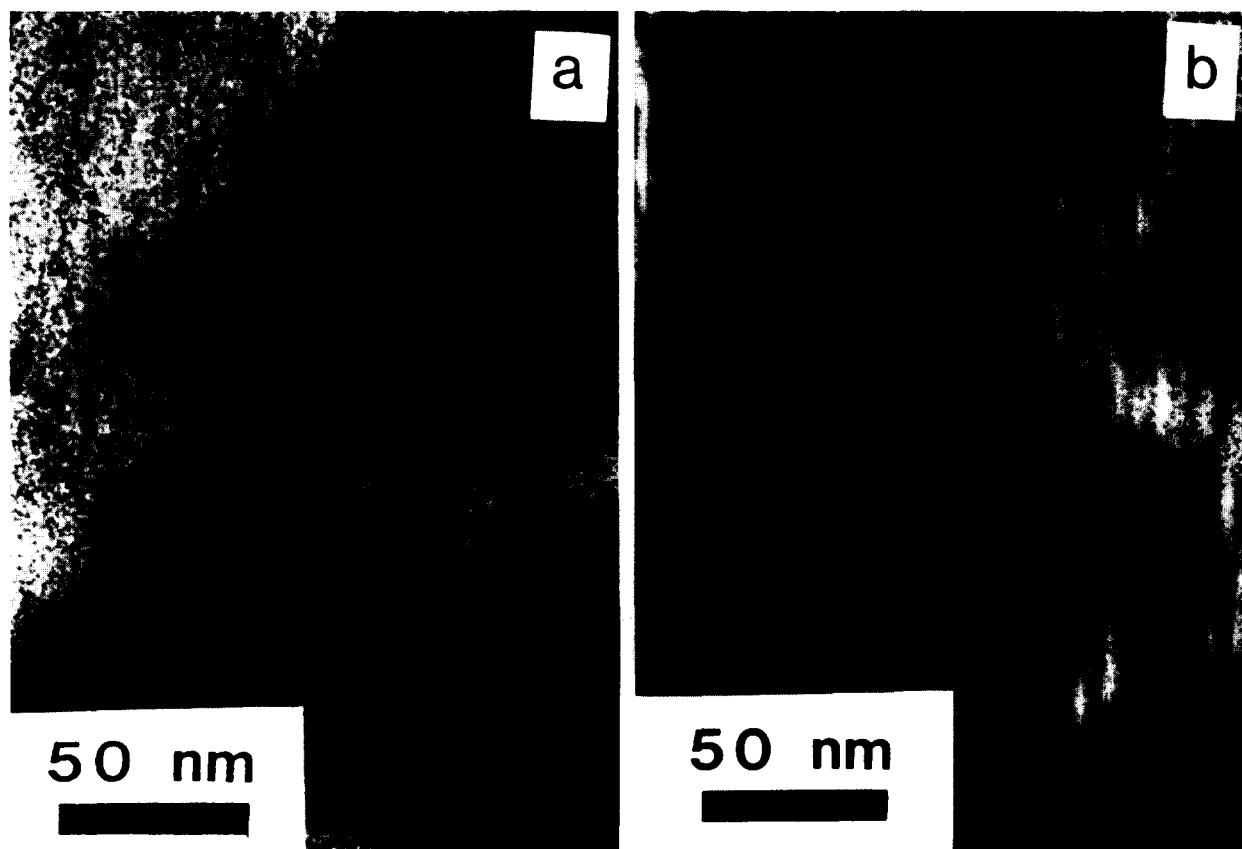


Figure 6. Electron micrographs showing the microstructure of the oriented PBZO/PPA phases observed in replicas of the fracture surface of frozen samples: (a) the form I state; (b) the form II state

During fibre spinning, microfibrils of the form II crystal solvate may develop in the skin of the fibre by absorption of moisture in the air gap above the coagulation bath, or in the fibre core at early stages of diffusion of water.

In summary, this study has provided insight as to the different crystal solvate forms of PBZO/PPA, comparison of this system to PBZT/PPA indicating a weaker polymer-solvent interaction in the latter, and pointing out that microfibrils already develop in the form II crystal solvate phase. Many issues, however, remain unanswered. The detailed structure of the PBZO/PPA crystals and changes in the structure at different temperatures need to be clarified. Little is known about the structure of the PPA solvent in the different phases, its conformation and degree of polymerization. There is no firm evidence for the point in a fibre-spinning process at which the microfibrillar morphology sets in and the mechanism by which the microfibrils form. Finally, whether the size of the microfibrils can be controlled by processing via crystal solvate phases, so as to enhance the properties of the PBZO fibres, is yet to be tested.

#### ACKNOWLEDGEMENTS

Y.C. gratefully acknowledges financial support by the US-Israel Binational Science Foundation and the US Air Force-European Office of Aerospace Research and Development. Y.C. also thanks the Polymer Branch, Wright Laboratory, for support as a visiting scientist and many helpful interactions.

#### REFERENCES

1 Adams, W. W., Eby, R. K. and McLemore, D. E. (Eds) 'The Materials Science and Engineering of Rigid-rod Polymers', Materials Research Society Symposium Proceedings, 1989, Vol. 134, Chapters 5 and 6

2 Wolfe, J. F., Loo, B. M. and Arnold, F. E. *Macromolecules* 1981, **14**, 915  
 3 Iovleva, M. M. and Papkov, S. P. *Polym. Sci. U.S.S.R.* 1982, **24**, 236; Papkov, S. P. *Adv. Polym. Sci.* 1983, **59**, 76  
 4 Cohen, Y. in 'The Materials Science and Engineering of Rigid-Rod Polymers' (Eds W. W. Adams, R. K. Eby and D. E. McLemore), Materials Research Society Symposium Proceedings, 1989, Vol. 134, p. 195  
 5 Cohen, Y., Saruyama Y. and Thomas, E. L. *Macromolecules* 1991, **24**, 1161  
 6 Cohen, Y., Buchner, S., Zachmann, H. G. and Davidov, D. *Polymer* 1992, **33**, 3811  
 7 Fratini, A. V. in 'The Materials Science and Engineering of Rigid-Rod Polymers' (Eds W. W. Adams, R. K. Eby and D. E. McLemore), Materials Research Society Symposium Proceedings, 1989, Vol. 134, p. 431  
 8 Martin, D. C. and Thomas, E. L. *Macromolecules* 1991, **24**, 2450  
 9 Adams, W. W., Kumar, S., Martin, D. C. and Shimamura, K. *Polym. Commun.* 1989, **30**, 285  
 10 Krause, S. J., Haddock, T. B., Vezie, D. L., Lenhart, P. G., W.-F. Hwang, Price, G. E., Helminiak, T. E., O'Brien, J. F. and Adams, W. W. *Polymer* 1988, **29**, 1354  
 11 Young, R. J., Day, R. J. and Zakikhani, M. *J. Mater. Sci.* 1990, **25**, 127  
 12 Cohen, Y. and Thomas, E. L. *Polym. Eng. Sci.* 1985, **25**, 1093  
 13 Cohen, Y. and Thomas, E. L. *Macromolecules* 1988, **21**, 433 and 437  
 14 Beltsios, K. G. and Carr, S. H. *J. Macromol. Sci.-Phys.* 1990, **B29**, 71  
 15 Feijoo, J. L., Odell, J. A. and Keller, A. *Polym. Commun.* 1990, **31**, 42  
 16 Based on molecular modeling using the Chem-X software, unpublished  
 17 Cohen, Y. and Cohen, E. *Macromolecules* 1995, **28**, 3631  
 18 Gardner, K. H., Matheson, R. R., Avakian, P., Chia, Y. T. and Gierke, T. D. *Polym. Prepr., ACS Polym. Chem. Div.* 1984, **23**, 469  
 19 Corbridge, D. E. C. *Acta Cryst.* 1956, **9**, 308  
 20 Jameson, R. F. in 'Phosphoric acid' Vol. 1, Part 2 (Ed. A. V. Slack), Marcel Dekker, New York, 1968  
 21 Roche, E. J. in 'The Materials Science and Engineering of Rigid-Rod Polymers' (Eds W. W. Adams, R. K. Eby and D. E. McLemore), Materials Research Society Symposium Proceedings, 1989, Vol. 134, p. 457  
 22 Roche, E. J., Allen, S. R., Gabara, V. and Cox, B. *Polymer* 1989, **30**, 1776